Nanoparticle Shape Evolution Identified through Multivariate Statistics

ARTICLE *in* THE JOURNAL OF PHYSICAL CHEMISTRY A · APRIL 2010

Impact Factor: 2.69 · DOI: 10.1021/jp100421t · Source: PubMed

6 AUTHORS, INCLUDING:

Subrata Kundu
Texas A&M University
94 PUBLICATIONS **3,061** CITATIONS
SEE PROFILE

Chiwoo Park
Florida State University
23 PUBLICATIONS **130** CITATIONS
SEE PROFILE

Hong Liang
Texas A&M University
222 PUBLICATIONS **2,002** CITATIONS
SEE PROFILE

Nanoparticle Shape Evolution Identified through Multivariate Statistics

David Huitink,[†] Subrata Kundu,[‡] Chiwoo Park,[§] Bani Mallick,[||] Jianhua Z. Huang,[||] and Hong Liang*,[†,‡]

Department of Mechanical Engineering, Materials Science and Engineering, Department of Industrial and Systems Engineering, Department of Statistics, Texas A&M University, College Station, Texas 77843

Received: January 15, 2010; Revised Manuscript Received: April 06, 2010

Precise morphological control of nanoparticles (NPs) has been impeded by the lack of in situ techniques enabling the observation of instantaneous growth steps. Fundamentally, understanding in NP nucleation and growth kinetics has yet to achieve. In the present research, morphological characterization is demonstrated using a novel image detection statistical approach for gold NPs. This multivariate statistical technique enhances the recognition of NPs by successfully identifying their morphology in addition to their growth stages. Thermodynamic analysis of those stages is presented relating surface energies to the growth kinetics. Preferred growth of NPs was seen to take place on specific crystallographic surfaces in a correlated manner. Furthermore, the growth steps are dominated by the adsorption of surfactants and the local surface energies. The present approach enabled detailed observation of NP growth kinetics and can be applied to other metallic NPs.

Introduction

Through refinement of various techniques, the synthesis of metallic NPs has been made possible with moderate shape and size selectivity.[1−16] The high surface activity of those NPs has led to their widespread use as catalysts in various chemical reactions,[4−7] and other properties, such as optical scattering and absorption, have resulted in their use as sensing elements.[8,9] As a result of the size and shape dependent NP applications, the synthesis of such NPs has evolved into a type of art form, where researchers have employed techniques such as laser ablation,[17,18] radio frequency (RF) plasma,[19] and chemical methods[20−23] to produce nanosized cubes,[24−26] prisms,[27−29] rods,[30,31] chains,[32−34] and, more commonly, spheres. While many works have recorded the methods of preparation and the effects of varying certain parameters for the production of such NPs, few studies have elucidated the nature of their formation, and the factors that drive the nucleation process.

To understand mechanisms of crystal growth, it is important to know the crystal nature of NPs. Though the intended application was a multigrain structure formed from solidification, Weinberg et al. simulated the interactions of neighboring anisotropic crystal grains,[35] showing the expected growth for crystalline material in a way that might hold application for multigrained NPs. Riwotzki and Haase have found that the crystalline structure of YVO_4 behaved no differently than the bulk crystal using UV excited lanthanide ion dopants to observe crystal penetration, proving that the crystallinity of NPs has no intrinsic difference from the bulk material.[36] As such, it is reasonable to assume that crystalline nature of NPs is the same or similar to that observed in bulk crystals. Researchers have acknowledged the differences in properties with respect to crystal directions,[15,37,38] but these differences have been largely overlooked when considering the nucleation kinetics of NPs. In the present study, we used a nonconventional approach to investigate the principles behind nanofabrication of NPs. An evaluation of Au NPs (citrate and cetyl-trimethyl ammonium bromide (CTAB) capped) synthesized under wet chemistry methods has divulged the significance of surface energies in the formation of NPs and their ultimate shape. To characterize the morphological properties of NPs, a statistical approach is employed. Additionally, thermodynamic considerations explaining the energy requirement for the formation of such particles has been discussed using a modified form of the Gibbs−Thomson equation.

Experimental Methods

During wet-chemical synthesis of gold NPs, various shaped and sized particles were obtained by altering the molar ratio of metal ions and stabilizing agent during the synthesis process, resulting in spheres, prisms, and rods, like those shown in the Supporting Information. Though identical in composition, each shape exhibits a unique UV−vis spectral absorption band. As has been well studied, these differences make NPs excellent sensors based on the sensitivity of the absorption spectra to the size and shape of the particles; however, often common synthesis methods yield mixtures of the various shapes and sizes limiting their usefulness. This particle heterogeneity is typically attributed to local concentration differences of reactants in solution.

To develop better control of the synthesis process, a highly accurate quantitative measurement tool for classifying the size and shape of NPs was developed for studying the sensitivity of particle shape to input conditions. This method employs a multivariate statistical approach with a semisupervised learning procedure, embedding a Bayesian multiclass logistic regression method to analyze NPs and their boundaries based on high resolution TEM images. As pictorially represented in Figure 1a−d, an edge detection algorithm first determines the particle boundaries (Figure 1a,b), then finds the centroids of each closed area (represented in Figure 1c), for which the identified shapes are then classified into groups of similar shapes (Figure 1d). The detection algorithm then identifies the most probable shapes and separates any overlapping particles into individual shapes

* To whom correspondence should be addressed. Tel: 979-862-2623. Fax: 979-845-3081. E-mail: hliang@tamu.edu.
[†] Department of Mechanical Engineering.
[‡] Materials Science and Engineering.
[§] Department of Industrial and Systems Engineering.
[||] Department of Statistics.

10.1021/jp100421t
Published on Web 04/14/2010

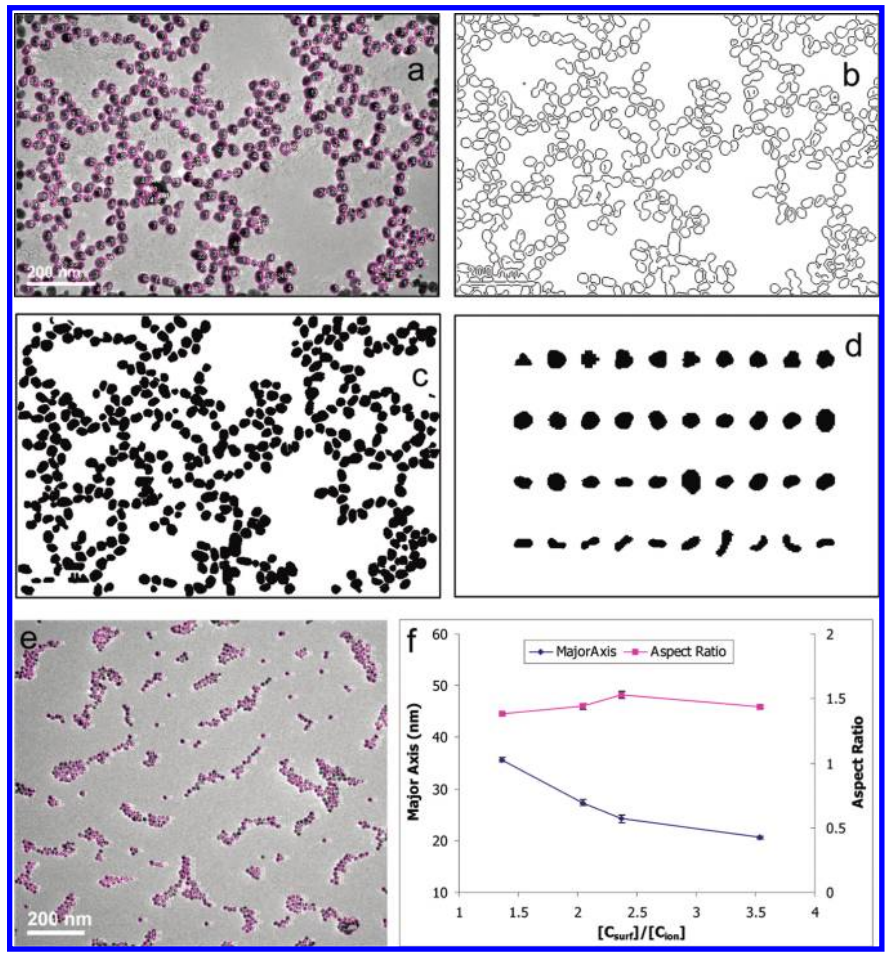

Figure 1. Description of advanced NP statistical analysis. From the original TEM image (a), particle boundaries are determined using edge detection (b) from which the shapes and centroids are identified (c). The shapes are then grouped by a correlation procedure (d) and used to further optimize the capture efficiency using probabilistic techniques. The final result allows for specific analysis of statistical features with high accuracy, even in the case of mild agglomeration (e). Further analysis revealing trend of major axis diameter and aspect ratio for multiple synthesis conditions (f).

of criteria which match the groupings identified in the previous step (Figure 1e). Using this method, a precise quantification of the size and shape statistics can be calculated and related to processing conditions, as exemplified in Figure 1f, where the major diameter and aspect ratio are plotted versus the ratio of citrate to gold ions (C_s/C_m) in one example using the Turkevitch method.[20] Using this method, we have observed shape capture efficiencies of 85−95%, compared to basic shape detection algorithms that have only captured between 15−45% of the particles (in the same images), without regard to separating overlapping NPs. Additionally, a subroutine of the algorithm can be used to identify color gradients that result from structural features inside the detected NPs.

Results/Discussion

Having seen the effects of the synthesis conditions upon the formation of various shapes or aspect ratios of NPs, it is important to consider the energy of formation for these varying conditions. To elucidate the thermodynamics concerning formation of NPs, typically the classical nucleation theory[39] is invoked, where the Gibbs free energy (ΔG) of the nucleating material is taken as

$$\Delta G = -\frac{4}{3}\pi r^3 \Delta G + 4\pi r^2 \gamma_{se} \quad (1)$$

Here, r is the radius of the nucleus, and ΔG_v and γ_{se} are the volumetric and surface energy, respectively, of the given material. The net effect of this theory reveals that there is a critical nucleus size, or threshold, that must be surpassed in order for a stable particle to exist and grow. This critical radius (r^*) is given as

$$r^* = 2(\gamma_{se}/\Delta G_v) \quad (2)$$

where the activation energy to form a stable nucleus is

$$\Delta G_a = \frac{16\pi \gamma_{se}^3}{3\Delta G_v^2} \quad (3)$$

This equation is restricted by two assumptions that differ from conditions in wet chemical synthesis. First, it assumes that the nucleation occurs in a homogeneous field of liquid of the same composition; and, second, it assumes that the resulting particle is spherical. For colloidal NP fabrication, both of these conditions are rescinded, as alternate shapes are evidenced and several heterogeneous chemical constituents are present including reducing agents, surfactants, and water or other solvents.[40−42] To satisfy the shape condition, a shape factor (ζ) is defined as

$$\zeta = R_v/R_s \quad (4)$$

where R_s and R_v are the equivalent surface area and equivalent volume spherical radii (i.e., defining a sphere of equal surface area or volume), respectively, such that the Gibbs nucleation equation can be alternatively represented in terms of the equivalent volume radius as

$$\Delta G = -\frac{4}{3}\pi {R_v}^3 \Delta G_v + 4\pi\left(\frac{R_v}{\zeta}\right)^2 \gamma_{se} \quad (5)$$

The shape factors (by definition, $\zeta \leq 1$) of some commonly observed NP shapes are listed in Supporting Information. Therefore, the critical radius of any shaped nuclei is thus calculated as

$$r^* = 2\frac{\gamma_{se}}{\Delta G_v}\frac{1}{\xi^2} \quad (6)$$

This indicates that the spherical shape, that is, $\zeta = 1$, represents the most stable system and the most likely shape to form as a NP embryo. Furthermore, based on this model alone, it is apparent that for the system to maintain the lowest energy configuration, it must be spherical.

Despite the apparent thermodynamic requirement for NPs to form spheres, they have been demonstrated to grow into many different shapes. It has been shown that by varying the concentration or composition of a stabilizing agent, different shapes of NPs result.[40−42] The ultimate particle may be expected to grow habitually from the "seed" geometry, as observed in crystal growth in larger scales.[43] Since NP nuclei thermodynamically favor spherical shape, then some transformation must take place to facilitate the formation of anisotropic NP seeds and their resultant particles. Justifiably, the anisotropic growth behavior of nonspherical NPs must have dependency on the crystal nature of metallic NPs. Kinetically speaking, one might expect that the highly packed facet, such as the [111] plane in face-centered cubic (fcc) structures, would require a longer time than crystalline surfaces which have lower area density.[44,45] Yet this does not explain all variations of shapes that may form; there must be an additional factor to result in the development of nonspherical particles. If we recall that crystalline materials, such as metals, have variations in surface energy depending on the exposed crystal face,[44,45] immediately we see that for the Gibbs−Thomson relationship the surface energy term is actually an averaged term. For example

$$\gamma_{se} = \frac{\sum_{i=1}^{\prime} \gamma_{se,i} A_i + \sum_{j=1}^{m} \gamma_{c,j} + \sum_{k=1}^{n} \gamma_{e,k}}{\sum_i A_i} \quad (7)$$

where the particle's net surface energy (γ_{se}) is the area average of the surface energy for each exposed crystal plane ($i = 1$, 2, 3, etc. corresponding to each planar face of the NP), including the energies corresponding to the exposed corners (γ_c) and edges (γ_e). As such, if the differences in the surface energies are sufficiently distinct, the particle will develop an anisotropic shape to reduce the overall surface energy.

Furthermore, the growth process is expected to have at least two competing factors, the deposition of gold atoms and the adsorption of surfactant molecules. Our experiments and others have proven that the resulting shape of the AuNPs depends on the concentration of surfactant. Moreover, an advanced edge detection analysis of TEM images of Au NPs produced using the Turkevitch method[20] found internal striations throughout the NP structures, indicating possible growth directions. Although the synthesis of NPs does not allow for in situ monitoring of their formation, these internal structural features may serve as evidence for their nucleation. A statistical analysis of these observations suggested that the directions of growth follow a bimodal distribution with respect to the long axis of the oblate semiellipsoidal NPs (Figure 2a). The two modes were identified

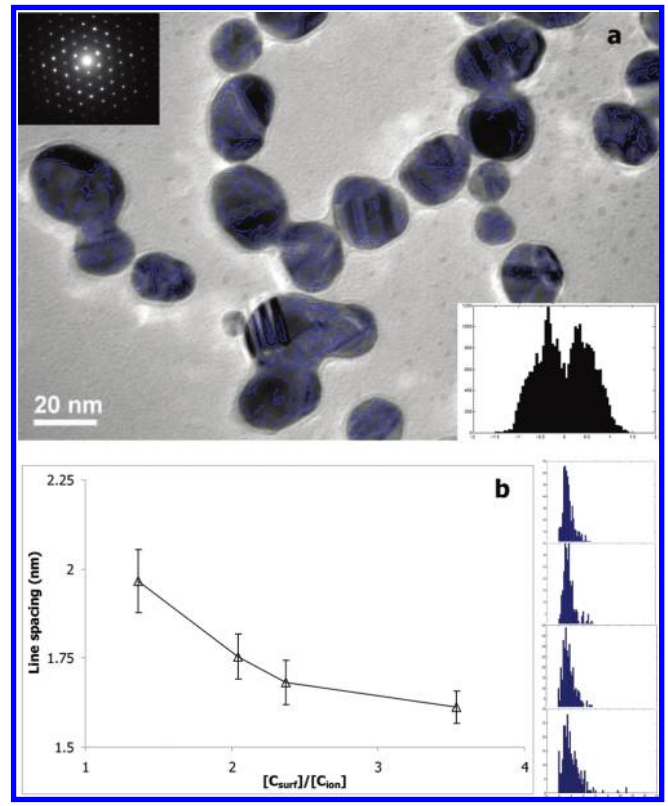

Figure 2. Internal striations detected in NPs reveal preferential orientations with respect to long axis of oblate particles (a) indicating growth directions. The average spacing between "parallel" lines (b) found to be related to concentration of surfactant present during synthesis, offering possible growth rate determination.

at ±0.4 radians, or ±22.9° (inset of the same figure). The angle observed between these two primary orientations happens to be the same 45° angle that exists between the (100) and (110) crystal planes, which are the two low packed (primary) surfaces for fcc gold. Regarding the surface energy differences, these lower packed planes (than the (111) plane) have a higher surface energy, which implies that higher energy planes favor the adsorption of metal ions onto those planes. Variations of surface energy are related to the planar density of surface atoms, and likewise, the number of "unpaired bonds," that is, the surface electron density. Similarly, the interactions between polar stabilizing molecules (like citrate or CTAB) and the NP surface are dominated by the electron density. NP shape formation is an energy driven process that is related to both physical and electronic characteristics at the surface of nucleation sites. The fact that charge and electron density can be experimentally manipulated via capping molecules allows for multiple possible shapes. For example, when investigating methods of NP shape purification, Khanal and Zubarev observed the reversible transformation of prismatic to round nanoplatelets.[46] The key factor was the introduction of either Au(III) with CTAB to prismatic shapes or Au(I) with CTAB and ascorbic acid. On these surfaces, the presence of either CTAB or CTAB and ascorbic acid disrupts the gold ion adsorption to either be isotropic or have planar dependencies, respectively. In fact, the dissolution of the larger prismatic shapes into isotropic spheres supports the concept of higher energy surfaces that are not stable without stabilizing agents. Kundu et al observed a transient ionization from Au(III) to Au(I) prior to forming NPs,[47] indicating that this transitional period may also affect ion migration onto the surface of the NPs.

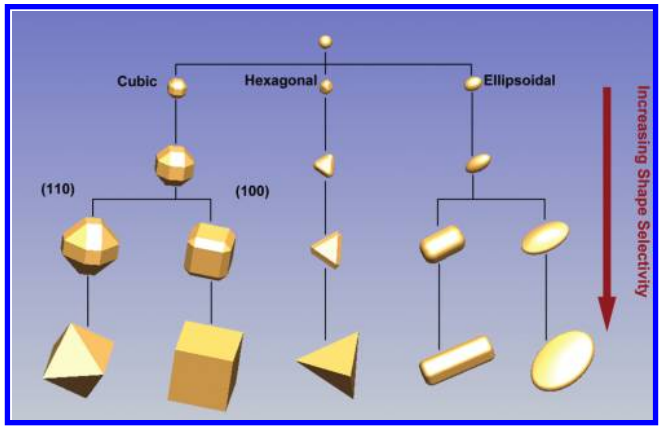

Figure 3. Schematic describing the effects of crystal planes and surfactant ordering on some possible shape configurations for metallic NPs.

A related phenomena was observed when evaluating the parallel lines inside each particle as measured by the developed algorithm. The median spacing was observed to increase from approximately 1 nm (with a positive skewed distribution), which is equal to approximately five (100) planes or four (110) planes, to 1.5 nm as the concentration ratio decreases (see Figure 2b). This may indicate a slowed growth rate along these crystal planes in the presence of higher surfactant concentrations.

Clearly, the surfaces and facets of the crystallographic nature of metal particles influences the growth and anisotropy seen in NPs. Ultimately, the shape donned by a given NP must minimize the net energy of the particle to maintain stability. Therefore, it would only make sense that for prismatic and other nonspherical shapes that the energies of the exposed planes, edges and corners must balance for an overall minimized condition. Since the energies of the corners are greater than the edges, and edges are greater than the surfaces, which differ from one another, there exists a configuration for which the total energy is minimized. The presence of surfactants can either alleviate these variations, leading to a spherical NP, or introduce other forms of anisotropy based on the ordered arrangement of the surfactant molecules themselves. This ordering may or may not be influenced by the crystal structure, based on the available number of sites to bond with the NP and dependent on the nature of the metal to surfactant molecule interaction. Furthermore, the surface electron density correlates strongly with the crystal arrangement which can significantly affect the binding of polar stabilizing agents. Once attaining a thermodynamically stable geometric configuration, the further adsorption of metal ions moderates the particle's habitual growth.

Essentially, the observation of growth mechanisms in NP synthesis in combination with an analysis of the nucleation thermodynamics has revealed that the NP embryos must initial exist as spheres. Once a stable nucleus is formed, the surface energy acts as the primary governing factor that determines the final shape. The further development of the shape is governed by the competition between the adsorption of surfactants and the deposition of atoms on low-density facets. This concept is schematically presented in Figure 3, where it provides a noncomprehensive shape evolution chart based on cubic and hexagonal crystal preferences as well as the influence of surfactant ordering. Although the provided results focus on AuNPs, the synthesis methods, parameters, and characterization techniques in developing the energy analysis transcend the example materials. As such, the theory can apply to other metallic NP systems synthesized using the reduction method.

Conclusions

Using novel experimental and statistical methods, the effect of crystallographic surfaces of NPs were seen to govern the actual formation of the particle. Evidence pointed to a complicated scheme of particle nucleation that traditional models do not explain. Thermodynamics requires that the particles take on certain forms after forming initial spherical nuclei to minimize the total system energy of the particle. Considering the Gibb-Thomson relation, it would appear that the formation of the nuclei must maintain sphericity, despite the crystal plane differences, leading to the conclusion that the NPs must exist in a fluid-like quasi-equilibrium prior to attaining the critical radius, which can only be maintained through the input of external energy (such as heat or irradiation). Furthermore, the presence and amounts of surfactants can alter the behavior and modify the growth rate. This analysis concerning nucleation and formation of Au NPs employed common techniques, but its principles can be applied to essentially any metallic particle formation in similar conditions. Ultimately, a fine-tuned understanding of this process can lead to the mass production of designed catalysts with high selectivity or particles of certain directional properties for use in nanocomposites, nanosensors, and many other potential applications.

Acknowledgment. The authors wish to acknowledge the financial support of the Norman Hackerman Advanced Research Program and the National Science Foundation Graduate Research Fellowship Program. We thank Dr. Yu Ding for discussions.

Supporting Information Available: A detailed description of the nanoparticle synthesis procedure as well as a further description of the image analysis algorithm is discussed in a supplemental file. Additionally, some calculations associated with the discussion of the modified Gibbs−Thomson equation are further explained. This material is available free of charge via the Internet at http://pubs.acs.org.

References and Notes

(1) Fendler, J. H.; Meldrum, F. C. The Colloid Chemical Approach to Nanostructured Materials. *Adv. Mater.* **1995**, *7* (7), 607–632.

(2) Schmid, G. Metals. In *Nanoscale Materials in Chemistry*; Klabunde, K. J., Ed.; Wiley: New York, 2001; pp 15−59.

(3) Toshima, N. Metal Nanoparticles for Catalysis. In *Nanoscale Materials*; 2003; pp 79−96.

(4) Valden, M.; Lai, X.; Goodman, D. W. Onset of Catalytic Activity of Gold Clusters on Titania with the Appearance of Nonmetallic Properties. *Science* **1998**, *281* (5383), 1647–1650.

(5) Kamat, P. V. Photophysical, Photochemical and Photocatalytic Aspects of Metal Nanoparticles. *J. Phys. Chem. B* **2002**, *106* (32), 7729–7744.

(6) Dawson, A.; Kamat, P. V. Semiconductor-Metal Nanocomposites. Photoinduced Fusion and Photocatalysis of Gold-Capped TiO_2 (TiO_2/Gold) Nanoparticles. *J. Phys. Chem. B* **2001**, *105* (5), 960–966.

(7) Troiani, H. E.; Camacho-Bragado, A.; Armendariz, V.; Gardea Torresday, J. L.; Jose Yacaman, M. Synthesis of Carbon Onions by Gold Nanoparticles and Electron Irradiation. *Chem. Mater.* **2003**, *15* (5), 1029–1031.

(8) Freibig, U.; Vollmer, M. *Optical Properties of Metal Clusters*; Springer-Verlag: New York, 1995.

(9) Elghanian, R.; Storhoff, J. J.; Mucic, R. C.; Letsinger, R. L.; Mirkin, C. A. Selective Colorimetric Detection of Polynucleotides Based on the Distance-Dependent Optical Properties of Gold Nanoparticles. *Science* **1997**, *277* (5329), 1078–1081.

(10) Paciotti, G. F.; Myer, L.; Weinreich, D.; Goia, D.; Pavel, N.; McLaughlin, R. E.; Tamarkin, L. Colloidal gold: a novel nanoparticle vector for tumor directed drug delivery. *Drug Delivery* **2004**, *11* (3), 169–183.

(11) Alper, J.; Crespo, M.; Hamad-Schifferli, K. Release Mechanism of Octadecyl Rhodamine B Chloride from Au Nanorods by Ultrafast Laser Pulses. *J. Phys. Chem. C* **2009**, *113* (15), 5967–5973.

(12) Hayakawa, K.; Yoshimura, T.; Esumi, K. Preparation of Gold-Dendrimer Nanocomposites by Laser Irradiation and Their Catalytic Reduction of 4-Nitrophenol. *Langmuir* **2003**, *19* (13), 5517–5521.

(13) Rashid, M. H.; Bhattacharjee, R. R.; Mandal, T. K. Organic ligand-mediated synthesis of shape-tunable gold nanoparticles: an application of their thin film as refractive index sensors. *J. Phys. Chem. C* **2007**, *111* (27), 9684–93.

(14) Khanna, V. K. Nanoparticle-based sensors. *Def. Sci. J.* **2008**, *58* (5), 608–16.

(15) Ahmadi, T. S.; Wang, Z. L. Shape-controlled synthesis of colloidal platinum nanoparticles. *Science* **1996**, *272* (5270), 1924.

(16) Kundu, S.; Wang, K.; Liang, H. Size-Controlled Synthesis and Self-Assembly of Silver Nanoparticles within a Minute Using Microwave Irradiation. *J. Phys. Chem. C* **2008**, *113* (1), 134–141.

(17) Nichols, W. T.; Sasaki, T.; Koshizaki, N. Laser ablation of a platinum target in water. II. Ablation rate and nanoparticle size distributions. *J. Appl. Phys.* **2006**, *100* (11), 114912–1.

(18) Jin, Z.; Lan, C. Q. Nickel and cobalt nanoparticles produced by laser ablation of solids in organic solution. *Mater. Lett.* **2008**, *62* (10−11), 1521–4.

(19) Swaminathan, R.; Willard, M. A.; McHenry, M. E. Experimental observations and nucleation and growth theory of polyhedral magnetic ferrite nanoparticles synthesized using an RF plasma torch. **2006**, *54* (3), 807–816.

(20) Turkevitch, J.; Stevenson, P. C.; Hillier, J. Nucleation and Growth Process in the Synthesis of Colloidal Gold. *Discuss. Faraday Soc.* **1951**, *11*, 55–75.

(21) Yonezawa, T.; Toshima, N., Polymer-Stabilized Metal Nanoparticles: Preparation, Characterization and Applications. In *Advanced Functional Molecules and Polymers*; Nalwa, H. S., Ed.; Gordon & Breach: Reading, UK, 2001; Vol. 2, pp 65−86.

(22) Brust, M.; Walker, M.; Bethell, D.; Schiffrin, D. J.; Whyman, R. Synthesis of thiol-derivatised gold nanoparticles in a two-phase Liquid-Liquid system. *J. Chem. Soc., Chem. Commun.* **1994**, (7), 801–802.

(23) Li, X.-M.; Jong, M. R. d.; Inoue, K.; Shinkai, S.; Huskens, J.; Reinhoudt, D. N. Formation of gold colloids using thioether derivatives as stabilizing ligands. *J. Mater. Chem.* **2001**, *11* (7), 1919–1923.

(24) Kundu, S.; Maheshwari, V.; Sanjun, N.; Saraf, R. F. Polyelectrolyte mediated scalable synthesis of highly stable silver nanocubes in less than a minute using microwave irradiation. *Nanotechnology* **2008**, *19* (6), 065604.

(25) Shukla, N.; Chao, L.; Roy, A. G. Oriented self-assembly of cubic FePt nanoparticles. *Mater. Lett.* **2006**, *60* (8), 995–8.

(26) Kalishwaralal, K.; Deepak, V.; Ram Kumar Pandian, S.; Gurunathan, S. Biological synthesis of gold nanocubes from Bacillus licheniformis. *Bioresour. Technol.* **2009**, *100* (21), 5356–5358.

(27) Millstone, J. E.; Metraux, G. S.; Mirkin, C. A. Controlling the edge length of gold nanoprisms via a seed-mediated approach. *Adv. Funct. Mater.* **2006**, *16* (9), 1209–14.

(28) Lee, K. Y.; Kim, M.; Kwon, S. S.; Han, S. W. Self-assembled silver nanoprisms monolayers at the liquid/liquid interface. *Mater. Lett.* **2006**, *60* (13−14), 1622–1624.

(29) Cui, B.; Clime, L.; Li, K.; Veres, T. Fabrication of large area nanoprism arrays and their application for surface enhanced Raman spectroscopy. *Nanotechnology* **2008**, *19* (14), 145302. 6 pp.

(30) Uthirakumar, P.; Han, N.; Woo, S. H.; Suh, E.-K.; Hong, C.-H. Synthesis and optical properties of sword-like GaN nanorods clusters. *Curr. Appl. Phys.* **2009**, *9* (1 SUPPL.), S114–S117.

(31) Kitamura, K.; Yatsui, T.; Ohtsu, M.; Yi, G. C. Fabrication of vertically aligned ultrafine ZnO nanorods using metal-organic vapor phase epitaxy with a two-temperature growth method. *Nanotechnology* **2008**, *19* (17), 175305. 3 pp.

(32) Yang, Y.; Shi, J.; Tanaka, T.; Nogami, M. Self-assembled silver nanochains for surface-enhanced Raman scattering. *Langmuir* **2007**, *23* (24), 12042–12047.

(33) Pendleton, A.; Kundu, S.; Liang, H. Controlled synthesis of titanium nanochains using a template. *J. Nanopart. Res.* **2009**, *11* (2), 505–510.

(34) Fei, X.; Hong-Guo, L.; Chang-Wei, W.; Yong-Ill, L.; Qingbin, X.; Xiao, C.; Jingcheng, H. Synthesis and assembly of ordered nanostructures of ZnS, ZnxCd1-xS and CdS nanoparticles at the air/water interface. *Nanotechnology* **2007**, *18* (43), 435603. 9 pp.

(35) Weinberg, M. C.; Birnie, D. P.; Farias, V. F. Simulation of Anisotropic Particle Shape Development during 2D Transformation. *J. Phys. Chem. B* **2002**, *106* (33), 8318–8325.

(36) Riwotzki, K.; Haase, M. Wet-Chemical Synthesis of Doped Colloidal Nanoparticles: YVO4:Ln (Ln = Eu, Sm, Dy). *J. Phys. Chem. B* **1998**, *102* (50), 10129–10135.

(37) Petroski, J. M.; Wang, Z. L.; Green, T. C.; El-Sayed, M. A. Kinetically Controlled Growth and Shape Formation Mechanism of Platinum Nanoparticles. *J. Phys. Chem. B* **1998**, *102* (18), 3316–3320.

(38) Yang, W.; Parr, R. G. Hardness, softness, and the fukui function in the electronic theory of metals and catalysis. *Proc. Natl. Acad. Sci. U.S.A.* **1985**, *82* (20), 6723–6726.

(39) Gibbs, J. W. *The Collected Works of J. W. Gibbs*, 2nd ed.; Pergamon: Warrendale, PA, 1975.

(40) Jana, N. R.; Gearheart, L.; Murphy, C. J. Evidence for Seed-Mediated Nucleation in the Chemical Reduction of Gold Salts to Gold Nanoparticles. *Chem. Mater.* **2001**, *13* (7), 2313–2322.

(41) Kundu, S.; Lau, S.; Liang, H. Shape-Controlled Catalysis by Cetyltrimethylammonium Bromide Terminated Gold Nanospheres, Nanorods, and Nanoprisms. *J. Phys. Chem. C* **2009**, *113* (13), 5150–5156.

(42) Kundu, S.; Wang, K.; Liang, H. Size-selective synthesis and catalytic application of polyelectrolyte encapsulated gold nanoparticles using microwave irradiation. *J. Phys. Chem. C* **2009**, *113* (13), 5157–5163.

(43) Reddy, E. S.; Babu, N. H.; Shi, Y.; Cardwell, D. A. Effect of size, morphology and crystallinity of seed crystal on the nucleation and growth of single grain Y-Ba-Cu-O. *J. Eur. Ceram. Soc.* **2005**, *25* (12), 2935–2938.

(44) Vitos, L.; Ruban, A. V.; Skriver, H. L.; Kollár, J. The surface energy of metals. *Surf. Sci.* **1998**, *411* (1−2), 186–202.

(45) Che, J. G.; Chan, C. T.; Jian, W. E.; Leung, T. C. Surface atomic structures, surface energies, and equilibrium crystal shape of molybdenum. *Phys. Rev. B* **1998**, *57* (3), 1875.

(46) Khanal, B. P.; Zubarev, E. R. Purification of High Aspect Ratio Gold Nanorods: Complete Removal of Platelets. *J. Am. Chem. Soc.* **2008**, *130* (38), 12634–12635.

(47) Kundu, S.; Pal, A.; Ghosh, S. K.; Nath, S.; Panigrahi, S.; Praharaj, S.; Pal, T. A New Route to Obtain Shape-Controlled Gold Nanoparticles from Au(III)-Î²-diketonates. *Inorg. Chem.* **2004**, *43* (18), 5489–5491.

JP100421T